Contents lists available at ScienceDirect

Physica B

journal homepage: www.elsevier.com/locate/physb

Electronic and annealing properties of the $E_{0.31}$ defect introduced during Ar plasma etching of germanium

F.D. Auret *, S.M.M. Coelho, G. Myburg, P.J. Janse van Rensburg, W.E. Meyer

Department of Physics, University of Pretoria, Pretoria, South Africa

ARTICLE INFO

PACS:
61.72.J –
61.72.uf
61.82. – d
66.30.Lw

Keywords:
Germanium
Ar plasma etching
Defects
DLTS
Annealing

ABSTRACT

Low energy (±80 eV) Ar plasma etching has been successfully used to etch several semiconductors, including GaAs, GaP, and InP. We have studied the only prominent defect, $E_{0.31}$, introduced in n-type Sb-doped Ge during this process by deep level transient spectroscopy (DLTS). The $E_{0.31}$ defect has an energy level at 0.31 eV below the conduction band and an apparent capture cross-section of 1.4×10^{-14} cm^2. The fact that no V–Sb defects and no interstitial-related defects were observed implies that the etch process did not introduce single vacancies or single interstitials. Instead it appears that higher order vacancy or interstitial clusters are introduced due to the large amount of energy deposited per unit length along the path of the Ar ions in the Ge. The $E_{0.31}$ defect may therefore be related to one of these defects. DLTS depth profiling revealed the $E_{0.31}$ concentration had a maximum (6×10^{13} cm^{-3}) close to the Ge surface and then it decreased more or less exponentially into the Ge. Finally, annealing at 250 °C reduced the $E_{0.31}$ concentration to below the DLTS detection limit.

1. Introduction

The low effective mass of holes in Ge has opened up the possibility of using Ge in ultrafast complimentary metal-oxide-semiconductor devices [1]. This, in turn, has sparked renewed interest in the properties of defects in Ge because defects ultimately determine the performance of devices. In recent studies the properties of the defects introduced during high energy gamma-, electron- and proton irradiation of Ge were reported [2–5]. We have reported the properties of defects introduced in Ge during electron beam deposition of various metals [6–8] and sputter deposition of Au [9]. However, no investigations regarding the defects introduced in Ge during surface cleaning processes, e.g. sputter and plasma etching, have been reported yet. These investigations are important because it is well known that the low energy ions utilized in these processes introduces defects at and close to the metal-semiconductor junction [10]. These defects influence device performance and alter the barrier heights of the contacts [6–9]. The defects responsible for these barrier adjustments are formed when energetic particles strike the semiconductor surface and interact with the semiconductor.

In this study we report the electronic properties of defects introduced in n-type Ge during low energy (±80 eV) inductively coupled plasma (ICP) Ar etching. We show that this process introduces only one prominent electron trap with an energy level at $E_C - 0.31$ eV. It is noteworthy that no defects involving single vacancies and interstitials were introduced by ICP etching.

2. Experimental procedure

We have used bulk-grown (111) n-type material doped with Sb to a level of 2.5×10^{15} cm^{-3} for this experiment. The samples were first degreased and then etched in a mixture of H_2O_2:H_2O (1:5, 30% H_2O_2) for 1 min. Directly after cleaning they were inserted into a vacuum chamber where AuSb (0.6% Sb) was resistively deposited on their back surfaces. The samples were then annealed at 350 °C in Ar for 10 min to obtain low resistivity ohmic contacts. Next, four samples were etched in an inductively coupled plasma (ICP) for times as indicated in Table 1. On three of the samples Pd contacts, 0.60 mm in diameter and 100 nm thick, were deposited (without breaking vacuum) using electron beam deposition (EBD) in the same vacuum chamber containing the ICP etcher. On the fourth, sample Pd Schottky contacts were deposited by resistive evaporation after ICP etching. It is well known that resistive evaporation does not introduce any defects in semiconductors. "Control" Pd Schottky contacts (no etching) were deposited on identical samples by resistive evaporation. Conventional deep level transient spectroscopy (DLTS) was used to study the defects introduced in the Ge during the ICP etch process.

---

* Corresponding author.
E-mail address: danie.auret@up.ac.za (F.D. Auret).

0921-4526/$ - see front matter © 2009 Elsevier B.V. All rights reserved.
doi:10.1016/j.physb.2009.09.028

Please cite this article as: F.D. Auret, et al., Physica B (2009), doi:10.1016/j.physb.2009.09.028

Table 1
Sample preparation.

Sample	Plasma etching (10 min)	Electron beam deposition	Resistive evaporation
a	No	No	Yes
b	No	Yes	No
c	Yes	No	Yes
d	Yes	Yes	No

3. Results and discussion

In Fig. 1 we depict the DLTS spectra for the control sample (curve (a)), for a sample with Pd contacts deposited by EBD without ICP etching (curve (b)), a sample that received a 10 min. ICP etch followed by resistive deposition of Pd contacts (curve (c)) and a sample that received a 10 min. ICP etch followed by EBD Pd contacts (curve (d)). Curve (a) clearly indicates that this material does not contain electron traps in measurable concentrations. The traps introduced in the Ge during EBD of Pd contacts (no ICP etching) are shown by curve (b). The two main traps are an electron trap, $E_{0.38}$, and a hole trap, $H_{0.30}$. In the nomenclature used here "E" and "H" mean electron and hole trap, respectively, and the subscripts are the activation energies determined from the Arrhenius plots in Fig. 2. These two levels have been shown to be related to the (−/-) and (-/0) charge states, respectively, of the E-center (V–Sb) in Sb-doped Ge [2,3] and have also previously been observed after EBD of Schottky contacts to Ge [6–8]. Evidently, the EBD process introduces vacancies in the Ge, at and close to the interface, that migrate and combine with, among others, Sb atoms to form Sb–V pairs. These vacancies have been proposed to be the result of energetic particles that originate in the region of the filament and then impinge on the semiconductor [11]. For comparison, we have also shown (in Fig. 2) the Arrhenius plots of the electron trap, $E_{0.38}$, and hole trap, $H_{0.30}$, associated with the E-center, as observed in a Ge sample that was irradiated with MeV electrons from a Sr^{90} radio-nuclide source. Whereas the plots for the $E_{0.38}$ align almost perfectly, there is a slight shift between the plots for the $H_{0.30}$ levels, that corresponds to about 1 K temperature difference for a given emission rate.

From curve (c) we note that ICP etching introduced only one prominent defect, $E_{0.31}$. Its properties are included in Table 2. DLTS spectra recorded under hole injection conditions revealed that no hole traps were present in this sample. It is instructive to note that no V–Sb centers or interstitial related defects [2,3] are introduced during the plasma etching of Ge. This implies that no single vacancies or interstitials were created at and below the Ge surface that could diffuse into the Ge to form the E-center. Alternatively, they were introduced at and near the surface but their migration into the Ge was impeded. This latter scenario is perhaps the most plausible because curve (d) shows that, although the contacts were deposited by EBD after ICP etching, the sample still only contains the $E_{0.31}$ defect. In this case no vacancies were injected into the Ge to form the E-center. From Fig. 2 it is also clear that the DLTS "signature" of the $E_{0.31}$ introduced by ICP etching is very different from the $E_{0.31}$ defect introduced by high-energy electron irradiation, indicating that they may be physically different defects.

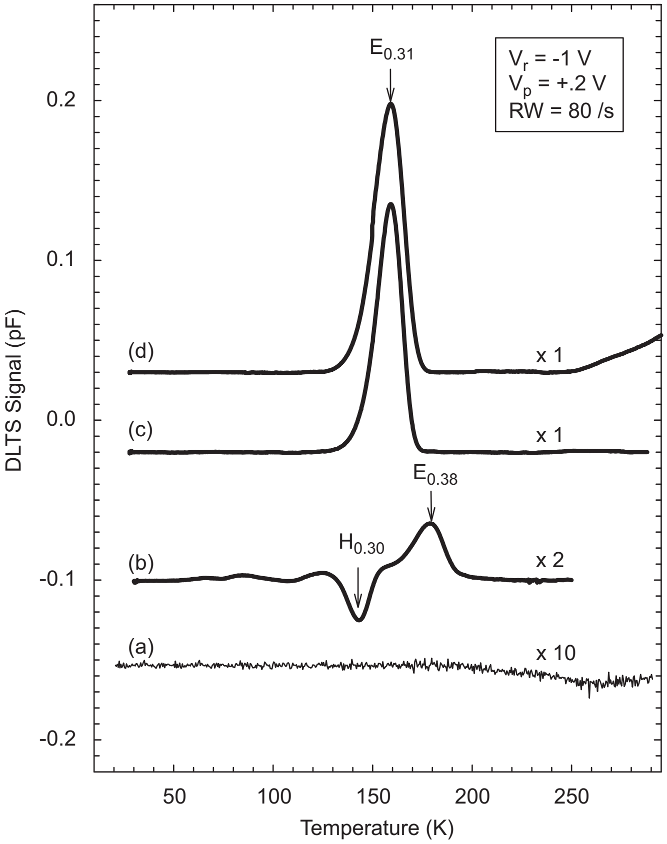

Fig. 1. DLTS spectra of resistively deposited (control) Pd Schottky contacts to n-Ge (curve (a)), of Pd Schottky contacts deposited by EBD (curve (b)), plasma etched Ge with resistively deposited Pd contacts (curve (c)) and plasma etched Ge with electron beam deposited Pd contacts (curve (d)). All spectra were recorded using a rate window of $80\,s^{-1}$ at a quiescent reverse bias of -1 V. For the electron-trap spectra the pulse, V_p, was 0.15 V into forward bias. Hole-trap spectra were obtained by applying an injection pulse of $V_p = 3$ V into forward bias.

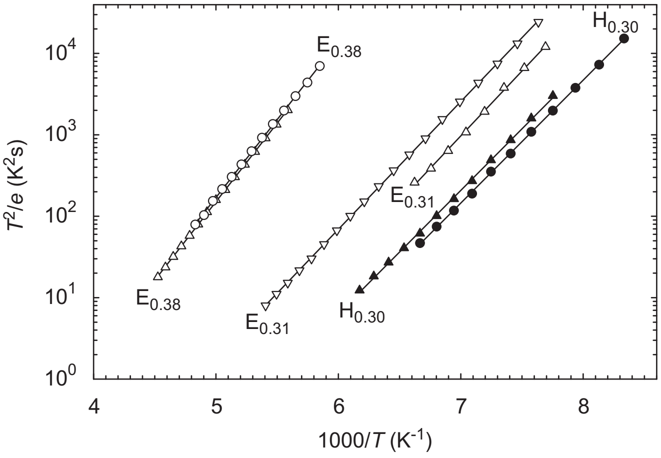

Fig. 2. Arrhenius plots traps introduced in n-type Ge by electron beam deposition (circles), high energy electron irradiation from a Sr^{90} radio-nuclide source (up triangles) and plasma etching (down triangles). Electron traps are indicated with empty symbols and hole traps by solid symbols. All data was acquired using the bias and pulsing conditions defined in the caption of Fig. 1.

We have used the fixed-bias variable pulse DLTS method to obtain the spatial distribution of the EBD and ICP etched induced defects into the Ge. From Fig. 3 we see that the $E_{0.31}$ defect is distributed much deeper (up to beyond one μm) into the Ge than the $E_{0.38}$ introduced by EBD. Furthermore, $E_{0.31}$ is significantly deeper into the Ge when the Schottky contact is deposited afterwards by EBD. This may be defect annealing due to sample heating during the EBD process.

Finally, we have performed isochronal annealing (10 min periods, 25 °C intervals) to establish the thermal stability of

Please cite this article as: F.D. Auret, et al., Physica B (2009), doi:10.1016/j.physb.2009.09.028

Table 2
Electronic properties of some prominent defects introduced in n-type Ge during plasma etching, Pd electron beam deposition and MeV electron irradiation.

Process	Defect	E_T (eV)	σ_a (cm^2)	T_{peak}[a] (K)	Similar defects/defect ID
Plasma etching	$E_{0.31}$	$E_C-0.31$	1.4×10^{-14}	156	–
EBD	$E_{0.38}$	$E_C-0.38$	1.0×10^{-14}	191	$E_{0.377}$[b], $E_{0.37}$[c], V–Sb (–/-)[b,c]
MeV	$H_{0.30}$	$E_V+0.30$	6.2×10^{-13}	141	$H_{0.307}$[b], $H_{0.30}$[c], V–Sb (-/0)[b]
Electron	$E_{0.38}$	$E_C-0.38$	1.1×10^{-14}	191	$E_{0.377}$[b], $E_{0.37}$[c], V–Sb (–/-)[b,c]
Irradiation	$H_{0.30}$	$E_V+0.30$	3.66×10^{-13}	142	$H_{0.307}$[b], $H_{0.30}$[c], V–Sb (-/0)[b]

[a] Peak temperature at a rate window of 80 s^{-1}.
[b] See Ref. [3].
[c] See Ref. [2].

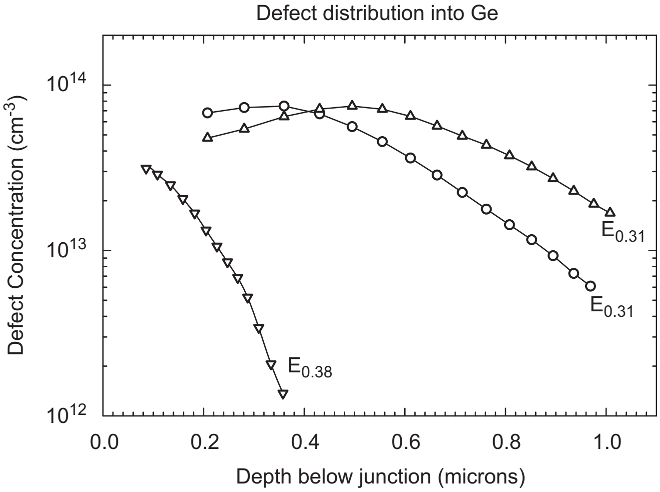

Fig. 3. DLTS depth profiles for the E-center ($E_{0.38}$) introduced by electron beam deposition (down triangles), the $E_{0.31}$ defects by plasma etching followed by resistive deposition of Pd (circles) and the $E_{0.31}$ defect introduced by plasma etching followed by electron beam deposition of Pd contacts (up triangles).

$E_{0.31}$. The DLTS measurements showed that the $E_{0.31}$ concentration remained constant up to 100 °C. Upon annealing at higher temperatures its concentration gradually decreased with increasing annealing temperature until it annealed out at 250 °C. By comparison, we have found that the E-center introduced by EBD in the same material annealed out at 225 °C.

4. Conclusions

Our results revealed that ICP Ar etching introduced only one detectable electron trap defect, $E_{0.31}$, in n-type Ge. This defect has not been observed in high energy electron irradiated Ge or after typical processing steps such as electron beam deposition, sputter deposition and ion implantation. DLTS depth profiling indicated that this defect could be detected even beyond one μm below the Pd–Ge interface. This is significantly deeper than the E-center introduced during electron beam deposition that could be detected only up to 0.4 μm below the interface in same material. The fact that no vacancy- or interstitial-related defects was detected after plasma etching (e.g. the V–Sb center) implies either that no single vacancies or interstitials are introduced, or that their migration into the Ge is impeded during the plasma etching.

EBD also introduced several defects that are not introduced by electron irradiation. Since EBD defects are introduced by heavy metal or gas ions, these defects could possibly be higher order vacancy clusters and complexes thereof with impurities. Annealing at 325 °C removed all the defects introduced during EBD of Pt Schottky contacts.

Acknowledgement

The authors gratefully acknowledge financial support of the South African National Research Foundation.

References

[1] Germanium Silicon: Physics and Materials, Semiconductors and Semimetals Vol. 56, R. Hull, J.C. Bean (Eds.), Academic Press, San Diego, 1999.
[2] J. Fage-Pedersen, A. Nylandsted Larsen, A. Mesli, Phys. Rev. B 62 (2000) 10.
[3] V.P. Markevich, A.R. Peaker, V.V. Litvinov, V.V. Emstev, L.I. Murin, J. Appl. Phys. 95 (2004) 4078.
[4] V.P. Markevich, I.D. Hawkins, A.R. Peaker, K.V. Emstev, V.V. Emstev, V.V. Litvinov, L. Dobaczewski, Phys. Rev. B 70 (2004) 235213.
[5] V.P. Markevich, I.D. Hawkins, A.R. Peaker, V.V. Litvinov, L. Dobaczewski, J.L. Lindström, Appl. Phys. Lett. 81 (2002) 1821.
[6] F.D. Auret, W.E. Meyer, S. Coelho, M. Hayes, Appl. Phys. Lett. 88 (2006) 242110.
[7] F.D. Auret, W.E. Meyer, S. Coelho, M. Hayes, J.M. Nel, Mater. Sci. Semicond. Process. 9 (2006) 576.
[8] F.D. Auret, S.M.M. Coelho, M. Hayes, W.E. Meyer, J.M. Nel, Phys. Status Solidi (a) 205 (2008) 159.
[9] F.D. Auret, S. Coelho, W.E. Meyer, C. Nyamhere, M. Hayes, J.M. Nel, J. Electron. Mater. 36 (2007) 1604.
[10] P.N.K. Deenapanray, F.D. Auret, G. Myburg, J. Vac. Sci. Technol. B 16 (1998) 1873.
[11] C. Christensen, J.W. Petersen, A. Nylandsted, Larsen, Appl. Phys. Lett. 61 (1992) 1426.

Please cite this article as: F.D. Auret, et al., Physica B (2009), doi:10.1016/j.physb.2009.09.028